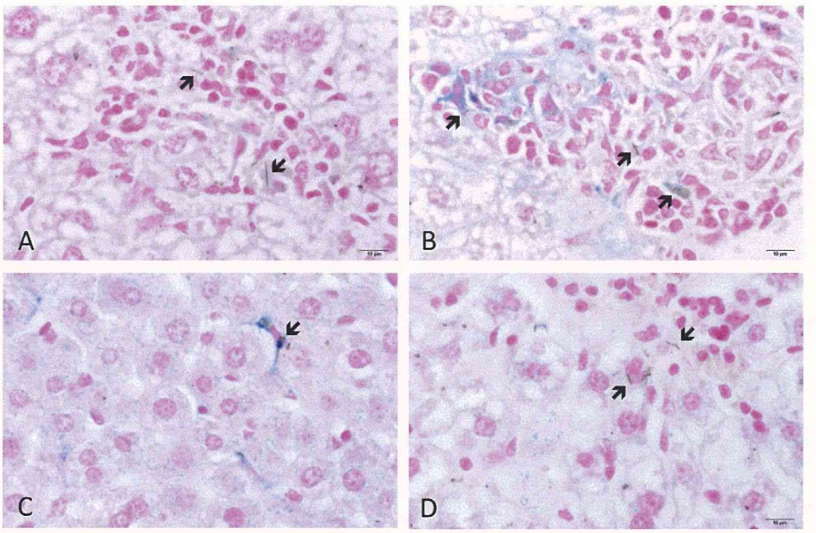

Fig. 6. Berlin blue staining (Fe^{3+} staining) of livers. A, A/J mice (Group 1); B, ICR mice (Group 2); C, C3H/HeN mice (Group 3); D, C57BL/6 mice (Group 4). The magnification is 1000× (A–D). Arrows indicate the fiber(s). Areas positive for Fe^{3+} were observed around the fibers rather than in focal lymphocyte infiltration itself (A–D). In the C3H/HeN case (Group 3), note several positive spots with fibers despite limited lymphocyte infiltration into the liver (C).

very low iron content (0.01%), on the accumulation of iron and ferritin by alveolar macrophages (AMs). This study indicates that AMs accumulate iron and ferritin in response to both iron loading of the lungs with iron oxide exposure and lung inflammation induced by calcium tungstate exposure (Wesselius et al., 1996). Therefore, an iron component is clearly not an absolute necessity. Iron is typically in the Fe^{3+} form in vivo and will need to be reduced prior to any Fenton activity and lung lining fluid contains antioxidants, such as glutathione and ascorbic acid, which can reduce Fe^{3+}–Fe^{2+} (Ruda and Dutta, 2005). These reports support that, in the present experiment, there have not been observed any positive spots for TurnBull's blue staining (for Fe^{2+}).

In the present experiment, lymphocyte infiltration into thickened pleura was remarkable in the lungs of ICR mice (Group 2) (Fig. 1D) and livers of A/J, ICR and C57BL/6, but not C3H/HeN, mice (Groups 1, 2 and 4) showed focal lymphocyte infiltration (Group 3), though fibers were present in all groups. From Berlin blue staining (for Fe^{3+}), regardless of whether the foci of lymphoid infiltration were large or not, Fe^{3+} positivity appeared to depend on the existence of the fibers. C3H/HeN mice (Group 3) showed several strong positive lesions for Fe^{3+} with the fibers, despite of the less of lymphocyte infiltration in the liver (Fig. 6C). It has been reported that cells of the immune system participate in the recognition and binding of iron as part of their postulated role in surveillance (Dorner et al., 1980). Iron bound to certain of the carrier molecules can enhance the proliferative response of lymphocytes to pokeweed mitogen (PWM) (Bryan and Leech, 1983) and iron modulates the expression of certain T lymphocyte surface markers (Nishiya et al., 1980a,b). The significance of the immuno-regulatory properties relates to a concomitant effect of iron on certain functional and structural aspects of cells involved in the immune response normal conditions as well as in an iron overload situation (Bryan et al., 1986). Therefore, iron concerns immuno-responses but, from the results of the present experiment, the reactivity for lymphocyte infiltration is suggested to vary from strain to strain.

To look overall, the histopathological findings in the lung, liver and kidneys are summarized in Table 3. The findings are variation depend on the strain and organs, and are seemed not to be consistency. For example, C3H/HeN mice showed strong Fe^{3+} positive lesions in the liver but not so strong in the lung. ICR mice showed strong lymphocyte infiltration in the pleura but not so strong in the liver. To explain the detail of between these differences and the risk in future, it is necessary for the longer experiment.

In conclusion, the present experiment demonstrated no unequivocal strain differences in the degree of the pleural thickening in response to TISMO fibers, but there was clear strain variation in iron and lymphocyte accumulation in the pleura and the liver. This in vivo information will likely be important when considering the development of mesothelioma in animal models, and in extrapolation to human risk. In order to obtain more detailed information on the relevance to malignancy, it is necessary that longer-term experiments now be conducted.

Conflict of interest

We have no conflicts of interest to be declared.

Acknowledgments

We thank Dr. Malcolm A. Moore for help in critical reading of this manuscript.

References

Alm AS, Li K, Chen H, Wang D, Andersson R, Wang X. Variation of lipopolysaccharide-induced acute lung injury in eight strains of mice. Respiratory Physiology & Neurobiology 2010;171:157–64.

Aung W, Hasegawa S, Furukawa T, Saga T. Potential role of ferritin heavy chain in oxidative stress and apoptosis in human mesothelial and mesothelioma cells: implications for asbestos-induced oncogenesis. Carcinogenesis 2007;28:2047–52.

Backus-Hazzard GS, Howden R, Kleeberger SR. Genetic susceptibility to ozone-induced lung inflammation in animal models of asthma. Current Opinion in Allergy and Clinical Immunology 2004;4:349–53.

Bryan CF, Leech SH. The immunoregulatory nature of iron. I. Lymphocyte proliferation. Cellular Immunology 1983;75:71–9.

Bryan CF, Leech SH, Bozelka B. The immunoregulatory nature of iron. II. Lymphocyte surface marker expression. Journal of Leukocyte Biology 1986;40:589–600.

Charles River Laboratories International I. Research animal models; 2012 http://www.criver.com/en-US/ProdServ/ByType/ResModOver/ResMod/Pages/CD-1Mouse.aspx

Crosby LM, Morgan KT, Gaskill B, Wolf DC, DeAngelo AB. Origin and distribution of potassium bromate-induced testicular and peritoneal mesotheliomas in rats. Toxicologic Pathology 2000;28:253–66.

Dorner MH, Silverstone A, Nishiya K, de Sostoa A, Munn G, de Sousa M. Ferritin synthesis by human T lymphocytes. Science 1980;209:1019–21.

Friedrichs KH, Molik B. Microscopic observations on some fibrous dust samples. Zentralblatt fur Bakteriologie, Mikrobiologie, und Hygiene Series B 1985;181:216–25.
Gong MN. Genetic epidemiology of acute respiratory distress syndrome: implications for future prevention and treatment. Clinics in Chest Medicine 2006;27:705–24.
Ikegami T, Tanaka A, Taniguchi M, Clark M, Ragan H, Mast T, et al. Chronic inhalation toxicity and carcinogenicity study on potassium octatitanate fibers (TISMO) in rats. Inhalation Toxicology 2004;16:291–310.
Ikegami T, Taniguchi M, Singer AW, Brooker MJ, Yarrington J, Placke ME, et al. Inhalation toxicity of potassium octatitanate fibers (TISMO) in rats following 13 weeks of aerosol exposure. Inhalation Toxicology 2000;12:415–38.
Jiang L, Nagai H, Ohara H, Hara S, Tachibana M, Hirano S, et al. Characteristics and modifying factors of asbestos-induced oxidative DNA damage. Cancer Science 2008;99:2142–51.
Jongsma J, van Montfort E, Vooijs M, Zevenhoven J, Krimpenfort P, van der Valk M, et al. A conditional mouse model for malignant mesothelioma. Cancer Cells 2008;13:261–71.
Kamp DW. Asbestos-induced lung diseases: an update. Translational Research 2009;153:143–52.
Kamstrup O, Ellehauge A, Collier CG, Davis JM. Carcinogenicity studies after intraperitoneal injection of two types of stone wool fibres in rats. Annals of Occupational Hygiene 2002;46:135–42.
Kim Y, Ton TV, DeAngelo AB, Morgan K, Devereux TR, Anna C, et al. Major carcinogenic pathways identified by gene expression analysis of peritoneal mesotheliomas following chemical treatment in F344 rats. Toxicology and Applied Pharmacology 2006;214:144–51.
Kleymenova EV, Horesovsky G, Pylev LN, Everitt J. Mesotheliomas induced in rats by the fibrous mineral erionite are independent from p53 alterations. Cancer Letters 1999;147:55–61.
Krajnow A, Lao I. Assessment of carcinogenic effect of aluminosilicate ceramic fibers produced in Poland. Animal experiments. Medycyna Pracy 2000;51:19–27.
Moore AJ, Parker RJ, Wiggins J. Malignant mesothelioma. Orphanet Journal of Rare Diseases 2008;3:34.
Nishiya K, Chiao JW, De Sousa M. Iron binding proteins in selected human peripheral blood cell sets: immunofluorescence. British Journal of Haematology 1980a;46:235–45.
Nishiya K, de Sousa M, Tsoi E, Bognacki JJ, de Harven E. Regulation of expression of a human lymphoid cell surface marker by iron. Cellular Immunology 1980b;53:71–83.
Page K, Lierl KM, Herman N, Wills-Karp M. Differences in susceptibility to German cockroach frass and its associated proteases in induced allergic inflammation in mice. Respiratory Research 2007;8:91.
Pauluhn J, Wiemann M. Siderite (FeCO(3)) and magnetite (Fe(3)O(4)) overload-dependent pulmonary toxicity is determined by the poorly soluble particle not the iron content. Inhalation Toxicology 2011;23:763–83.
Ruda TA, Dutta PK. Fenten chemistry of Fe(III)-exchanged zeolitic minerals treated with antioxidants. Environmental Science and Technology 2005;39:6147–52.
Sakamoto Y, Nakae D, Fukumori N, Tayama K, Maekawa A, Imai K, et al. Induction of mesothelioma by a single intrascrotal administration of multi-wall carbon nanotube in intact male Fischer 344 rats. Journal of Toxicological Sciences 2009;34:65–76.
Shield PW, Koivurinne K. The value of calretinin and cytokeratin 5/6 as markers for mesothelioma in cell block preparations of serous effusions. Cytopathology 2008;19:218–23.
Shimkin MB, Stoner GD. Lung tumors in mice: application to carcinogenesis bioassay. Advances in Cancer Research 1975;21:1–58.
Takagi A, Hirose A, Nishimura T, Fukumori N, Ogata A, Ohashi N, et al. Induction of mesothelioma in p53+/– mouse by intraperitoneal application of multi-wall carbon nanotube. Journal of Toxicological Sciences 2008;33:105–16.
Takeuchi H, Saoo K, Matsuda Y, Yokohira M, Yamakawa K, Zeng Y, et al. 8-Methoxypsoralen, a potent human CYP2A6 inhibitor, inhibits lung adenocarcinoma development induced by 4-(methylnitrosamino)-1-(3-pyridyl)-1-butanone in female A/J mice. Molecular Medicine Reports 2009;2:585–8.
Toyokuni S. Iron-induced carcinogenesis: the role of redox regulation. Free Radical Biology and Medicine 1996;20:553–66.
Toyokuni S. Elucidation of asbestos-induced carcinogenesis and its application to prevention, diagnosis and treatment in relation to iron. Japanese Journal of Lung Cancer 2009;49:362–7.
Toyokuni S. Mysterious link between iron overload and CDKN2A/2B. Journal of Clinical Biochemistry and Nutrition 2011;48:46–9.
Toyokuni S, Tanaka T, Hattori Y, Nishiyama Y, Yoshida A, Uchida K, et al. Quantitative immunohistochemical determination of 8-hydroxy-2′-deoxyguanosine by a monoclonal antibody N45.1: its application to ferric nitrilotriacetate-induced renal carcinogenesis model. Laboratory Investigation 1997;76:365–74.
Wagner JC, Skidmore JW, Hill RJ, Griffiths DM. Erionite exposure and mesotheliomas in rats. British Journal of Cancer 1985;51:727–30.
Wesselius LJ, Smirnov IM, Nelson ME, O'Brien-Ladner AR, Flowers CH, Skikne BS. Alveolar macrophages accumulate iron and ferritin after in vivo exposure to iron or tungsten dusts. Journal of Laboratory and Clinical Medicine 1996;127:401–9.
Yokohira M, Hashimoto H, Yamakawa K, Suzuki S, Saoo K, Kuno T, et al. Potassium octatitanate fibers (TISMO) induce pleural mesothelial cell reactions with iron accumulation in female A/J mice. Oncology Letters 2010;1:589–94.
Yokohira M, Hashimoto N, Yamakawa K, Saoo K, Kuno T, Imaida K. Lack of promoting effects from physical pulmonary collapse in a female A/J mouse lung tumor initiated with 4-(methylnitrosamino)-1-(3-pyridyl)-1-butanone (NNK) with remarkable mesothelial cell reactions in the thoracic cavity by the polymer. Experimental and Toxicologic Pathology 2011;63:181–5.
Yokohira M, Kuno T, Yamakawa K, Hashimoto N, Ninomiya F, Suzuki S, et al. An intratracheal instillation bioassay system for detection of lung toxicity due to fine particles in F344 rats. Journal of Toxicologic Pathology 2009;22:1–10.
Yokohira M, Takeuchi H, Yamakawa K, Saoo K, Matsuda Y, Zeng Y, et al. Bioassay by intratracheal instillation for detection of lung toxicity due to fine particles in F344 male rats. Experimental and Toxicologic Pathology 2007;58:211–21.

The Journal of Toxicological Sciences (J. Toxicol. Sci.)
Vol.38, No.4, 619-628, 2013

Original Article

An improved dispersion method of multi-wall carbon nanotube for inhalation toxicity studies of experimental animals

Yuhji Taquahashi, Yukio Ogawa, Atsuya Takagi, Masaki Tsuji, Koichi Morita and Jun Kanno

Division of Cellular and Molecular Toxicology, Biological Safety Research Center, National Institute of Health Sciences, 1-18-1 Kamiyoga, Setagaya-ku, Tokyo 158-8501, Japan

(Received May 5, 2013; Accepted June 9, 2013)

ABSTRACT — A multi-wall carbon nanotube (MWCNT) product Mitsui MWNT-7 is a mixture of dispersed single fibers and their agglomerates/aggregates. In rodents, installation of such mixture induces inflammatory lesions triggered predominantly by the aggregates/agglomerates at the level of terminal bronchiole of the lungs. In human, however, pulmonary toxicity induced by dispersed single fibers that reached the lung alveoli is most important to assess. Therefore, a method to generate aerosol predominantly consisting of dispersed single fibers without changing their length and width is needed for inhalation studies. Here, we report a method (designated as Taquann method) to effectively remove the aggregate/agglomerates and enrich the well-dispersed singler fibers in dry state without dispersant and without changing the length and width distribution of the single fibers. This method is base on two major concept; liquid-phase fine filtration and critical point drying to avoid re-aggregation by surface tension. MWNT-7 was suspended in Tert-butyl alcohol, freeze-and-thawed, filtered by a vibrating 25 μm mesh Metallic Sieve, snap-frozen by liquid nitrogen, and vacuum-sublimated (an alternative method to carbon dioxide critical point drying). A newly designed direct injection system generated well-dispersed aerosol in an inhalation chamber. The lung of mice exposed to the aerosol contained single fibers with a length distribution similar to the original and the Taquann-treated sample. Taquann method utilizes inexpensive materials and equipments mostly found in common biological laboratories, and prepares dry powder ready to make well-dispersed aerosol. This method and the chamber with direct injection system would facilitate the inhalation toxicity studies more relevant to human exposure.

Key words: Multi-wall carbon nanotube, Dispersion, Metallic sieve, Tert-butyl alcohol, Sublimation, Critical point drying

INTRODUCTION

We previously reported that a certain make of multi-wall carbon nanotube (MWCNT) contained particles similar to asbestos fibers in size and shape, and was positive for mesotheliomagenesis in intraperitoneal injection studies using p53-heterozygous mice (Takagi et al., 2008, 2012). The intraperitoneal injection study is a specialized method for the detection of mesotheliomagenic potential of inhaled fibrous materials (Pott et al., 1994; Roller et al., 1997; Poland et al., 2008). For the assessment of general respiratory toxicity including non-cancerous endpoints, the inhalation studies are considered essential. As a surrogate for inhalation studies, pharyngeal aspiration and intratracheal spray methods are often used. However, in both methods, the suspension medium may modify the distribution and/or the toxicity of the test particles (Morimoto et al., 2011; Oyabu et al., 2011; Gasser et al., 2012; Wang et al., 2012). Dispersion methods without suspension media are reported. However, those are usually using, at least in part of the processes, rigorous sonication or mechanical milling resulting in certain degree of physiological changes in sample characteristics, such as shortening in length distribution of MWNCT (Muller et al., 2005; Mitchell et al., 2007; Ahn et al., 2011). Changes in particle size and/or shape will also affect the nature

Correspondence: Jun Kanno (E-mail: kanno@nihs.go.jp)

and strength of toxicity of the test substances. Therefore, development of a dispersion method to generate the aerosol of concern without addition of chemicals and changes in particle dimensions is considered to be essential for the assessment of inhalation toxicity in humans.

Fibrous nanomaterial such as Mitsui MWNT-7 is a mixture of dispersed single fibers of various length and width, and their agglomerates and aggregates. When given as a mixture, the lung lesions were mainly seen as inflammatory and/or granulomatous lesions with various degree of fibrosis at the level of terminal bronchiole accompanying the aggregates and agglomerates. These lesions were considered to block and/or mask the changes induced by the single fibers that should have reached the alveolar ducts and alveoli (Warheit et al., 2004; Muller et al., 2005; Shvedova et al., 2008; Porter et al., 2009; Mercer et al., 2011; Wang et al., 2011). Therefore, assessment of the toxicity of single fibers needs well-dispersed sample without aggregate/agglomerate. In practical inhalation testing, the animal chamber air is rigorously agitated in order to ensure the homogeneity of aerosol in the chamber. Therefore, if the MWNT-7 as a mixture is used, the likelihood of aggregates/agglomerates reaching the nose of the animals is high. In contrast, human ambient air is less agitated; the aggregates/agglomerates may sediment away fast and dispersed single fibers may stay longer in the air to be inhaled by humans (Han et al., 2008). In addition, humans have longer respiratory tract compared to rodents and may effectively filtered out aggregates/agglomerates before the air reaches the alveolar region.

Taking all into account, we concluded that it is essential to prepare a dispersed single fiber aerosol without aggregate/agglomerates, without additional chemical components, and without changes in size and shape of the single fiber component for the rodent inhalation studies in order to predict human inhalation toxicity. To date, one dispersion method is reported, i.e. the filtration system. Filtration by a sieve with its pore size smaller than the size of aggregates/agglomerate will not affect the size distribution of the single fibers (Kasai et al., 2013). However, filtration in gaseous phase turns out to be ineffective in terms of yield of the filtrate. Filtration in liquid phase is much efficient (Mercer et al., 2008; Tsuda, personal communication). However, in our experience, the difficulty is found in avoiding re-aggregation during the process of drying; the surface tension. To solve this problem, here we report a new improved dispersion method consisting of a combination of aqueous filtering and the concept of a drying method used for scanning electron microscopic (SEM) samples; the critical point drying.

MATERIALS AND METHODS

MWCNT, reagent and equipments

MWCNT (Mitsui MWNT-7) was kindly donated by Mitsui & Co., Ltd., Tokyo, Japan for use in toxicity studies (Takagi et al., 2008). Tert-butanol (TB) of guaranteed reagent grade was used (CAS: 75-65-0, Kanto Chemical Co., Inc., Tokyo, Japan). Metallic Sieve (pore size 25 μm mesh, Seishin Enterprise Co., LTD., Tokyo, Japan) was used for filtration. Miniature coin type vibration motors used in cellular phones (Model FM34F, T.C.P. Co, Tokyo Japan; 13,000 rpm 1.8m²/sec) are attached to the extended filler rim (5cm in depth, custom-made, Seishin Enterprise Co., LTD.) of the metallic sieve (cf. Fig. 1c) to gain high yield of filtrate. Chemistry diaphragm pumps and pumping systems (Model; MD4C NT+AK+EK, Vacuubrand, Wertheim, Germany) was used for sublimation of the frozen TB suspension and recovery of TB. Glass wares such as funnel, filtering bottle, trap bottle and silicon stoppers (Sansyo Co., Ltd., Tokyo, Japan), laboratory bottles (Pyrex®, Asahi Glass Co. Ltd., Tokyo, Japan), were used.

Dispersion method ("Taquann" method)

An outline flowchart is shown in Fig. 1. TB (melting point 25.69°C) was heated up to 60°C by a mantle heater (Sibata Scientific Technology Ltd., Saitama, Japan). It is advised not to use water bath; TB is highly hygroscopic and becomes difficult to freeze and sublimate. A volume of 200 ml of TB and 0.2 g of MWCNT were transferred to a 500 ml laboratory bottle and agitated to make crude suspension. The bottle was put into an ice bath, occasionally shaken by hand, until the suspension starts to freeze and becomes sherbet-like half frozen state and kneaded by a stainless steel spatula until it becomes evenly gray without clear crystals of TB (Fig. 1a), and then kept overnight at -25°C. To the frozen suspension, 500 ml of TB pre-heated to 60°C, was added, capped and shaken hard until the liquefied suspension becomes evenly dark brown to gray in color (Fig. 1b). The bottle was further heated up to 60°C by a mantle heater and the suspension was immediately applied to vibrating metal sieve for filtration (Fig. 1c). The filtrate was collected through a funnel into a 1,000 ml laboratory bottle. Immediately after the filtration, approximately 1,500 ml of liquid nitrogen was poured onto the filtrate in the bottle to snap freeze the suspension (Fig. 1d). Then, the bottle was connected to the pumping system and vacuumed until TB was totally sublimated; leaving dispersed MWCNT (T-CNT for Taquann-treated MWCNT) in the bottle. The MWCNT was collected by a cyclone-suction bottle using conduc-

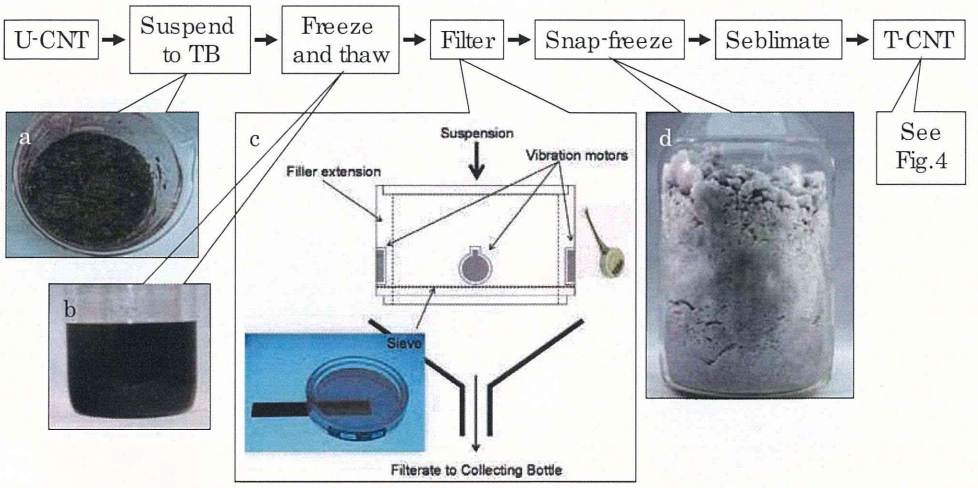

Fig. 1. Outline flowchart of the Taquann method. a) Half-frozen sherbet-like suspension of MWNT-7 kneaded (beaker was used for demonstration). b) Well-shaken liquefied suspension after adding 60°C TB (beaker was used for demonstration). c), Photograph of the sieve on a backlight box with a scale underneath (left inset), vibration motor (right inset), and a diagram of the filter unit with a filler extension and vibration motors. d) Snap-frozen filtrate.

tive silicon and aluminum tubing. In order to make a precise aliquot, a measured amount the collected T-CNT was resuspended to TB, and the suspension was aliquoted into proper containers, in this study into the newly designed cylindrical cartridge case (cf. Fig. 3), snap-frozen, and sublimated.

Aerosol generation system

An originally designed 105 L main exposure chamber (capacity of 16 mice per chamber), with a disposable electrostatic-free plastic bag inside, was prepared (Fig. 2, patent pending, manufactured by Sibata Scientific Technology Ltd.). Onto the plastic disposable top plate, a 20 L subchamber was connected with a 5 cm-diameter 10 cm long connecting pipe. To the subchamber, an injection port was connected, to which a newly designed cylindrical cartridge (manufactured by Sibata Scientific Technology Ltd.) containing dispersed T-CNT is loaded. The cartridge has a slide-valve air inlet at its base and four ejection holes at its top opening towards the subchamber lumen. The compressed air (0.8 M pascal) was injected five times with 0.2 sec duration and 10 sec interval to empty the T-CNT into the subchamber (Fig. 3). The carrier air flow from the subcamber to the main chamber was 15 L/min. Twenty-one cartridges were prepared for a two-hr exposure experiment, loading first two in 1 min for an initial boost and then one in every 6 min, resulting in generation of saw-tooth concentration wave with an average of 1.3 mg/m^3 (250 μg/cartridge) and 2.8 mg/m^3 (500 μg/cartridge).

Twelve C57BL/6NCrSlc male mice (SLC, Inc., Shizuoka, Japan), 10~11 weeks old, body weight of 23.8~30.8 g were placed in the cage suspended from the top plate of the inhalation chamber and exposed to 1 mg/m^3 of T-CNT for 2 hr a day for 5 days, lungs (excluding primary bronchi) were sampled and subjected to characterization of deposited fibers (see below).

The animal study was conducted in accordance with the Guidance for Animal Studies of the National Institute of Health Sciences under Institutional approval.

Real time particle counting and weight measurement

An optical particle counter (OPC) with a nominal detection limit of 300 nm (OPC-110GT, Sibata Scientific Technology Ltd.) and a condensation particle counter (CPC) with a nominal detection limit of 2.5 nm (ultrafine condensation particle counter 3776, Trust Science Innovation, MN, USA) were connected to the main chamber with a sample flow of 2.83 L (0.1cf) /min and 0.3 L/min respectively. The mass concentration of the chamber aerosol was calculated from the weight increase of polytetrafluoroethylene-glass fiber filter (Model T60A20, φ55mm, Tokyo Dylec Corp, Tokyo, Japan) after filtering the chamber aerosol by an Asbestos sampling pump (AIP-105, Sibata Scientific Technology Ltd.) at a rate of 1.5 L/min for 120 min (total of 180 L). Filter weight was measured by a microbalance (XP26V,

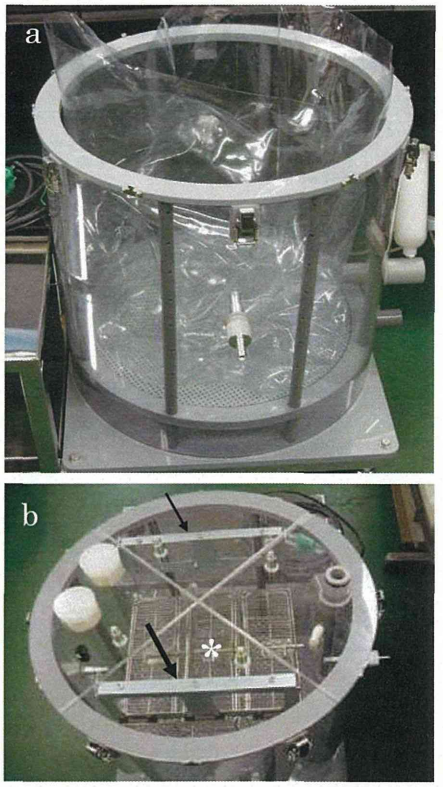

Fig. 2. Newly designed original inhalation chamber. a) Outer chamber and inner bag before top plate is in place. During operation, the space between the outer chamber and inner bag is negatively pressured to inflate the inner bag. B) Disposable top plate with tubing holes are placed on the chamber. The animal cages for 16 mice (asterisk) are suspended from the top place by a pair of hanger arms (arrows) (photo was taken without inner bag for better demonstration).

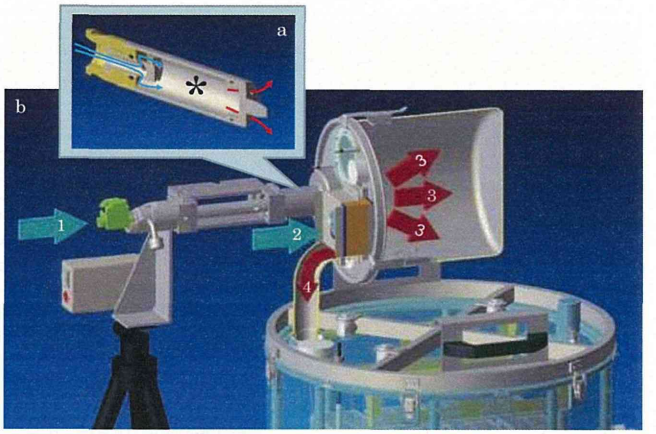

Fig. 3. A scheme of direct injection aerosol generation system. a) Upper inset shows the cut section of the injection cartridge (capacity; 23.5 ml). A slide valve opens when the cartridge is loaded to the subchamber. A measured amount of dispersed MWCNT is preloaded inside the cartridge shown in asterisk. b) Compressed air (Blue arrow 1) blows out the MWCNT through four small outlets of the cartridge into the subchamber (red arrows 3), where main flow air from the HEPA filtered inlet (blue arrow 2) mixes in. The air with the aerosol goes down the connection pipe to the main chamber (red arrow 4).

Mettler Toledo).

Characterization of the dispersed MWCNT

The T-CNT in TB suspension was mounted on a slide glass and observed under a light microscope using a pair of polarizing filters. Untreated MWCNT (U-CNT) from the bulk, 200 mg, was dispersed in to 500 ml of TB and sonicated for 30 min at 40W, 3.4 kHz (SU-3TH, Sibata Scientific Technology Ltd.) and observed.

A weight-measured aliquot of T-CNT was re-suspended, blotted on a Anopore™ Inorganic Aluminum Oxide Membrane Filters (Whatman GmbH, Dassel GE Healthcare, Hahnestrasse, Germany, pore size; 0.02 μm, φ13 mm, Anodisc 13) or a cellulose acetate/nitrocellulose membrane filter (MFTM- Millipore Membrane filters, 0.025 μm, φ13 mm, Merck Millipore, Billerica, MA, USA) and observed with a scanning electron microscope (SEM).

From the main chamber, the aerosol was collected at a rate of 5 L/min for 3 min on a Anopore™ Inorganic Aluminum Oxide Membrane Filters (Whatman GmbH, pore size; 0.1 um, Anodisc 25) joined to asbestos sampling pump (AIP-105, Sibata, Scientific Technology Ltd.). A scanning electron microscope (SEM) (VE-9800, Keyense Co., LTD., Osaka, Japan) was used for monitoring the details of the samples on the slide glasses and on the Anodiscs after osmium coating (HPC-1SW, Vacuum Device Inc., Ibaraki, Japan).

From the exposed mouse, lung lobes are collected and treated with lysis solution composed of 5 w/v% potassium hydroxide (Super Special Grade, Wako Pure Chemical Industries, Ltd., Osaka, Japan), 0.1w/v% Sodium dodecyl sulfate (SDS, for Biochemistry, Wako Pure Chemical Industries, Ltd.), 0.1 w/v% Ethylenediamine-N,N,N',N'-tetraacetic acid disodium salt dehydrate (EDTA 2Na, Dojindo laboratories, Kumamoto, Japan) and 2w/v% ascorbic acid (Super Special Grade, Wako Pure Chemical Industries, Ltd.) in ultra-pure water, dissolved at 80°C (Fig. 10b). Lung samples (approx. 200 mg) and 1.8 ml of

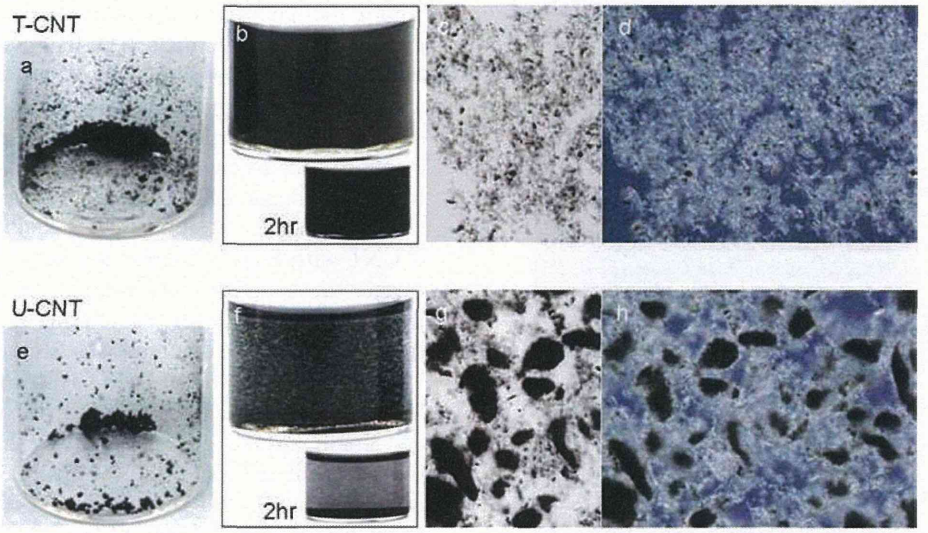

Fig. 4. Taquann-treated carbon nanotube (T-CNT) and untreated bulk carbon nanotube (U-CNT). a) final fine and dry powder of Taquann-treated MWCNT. b) Resuspended T-CNT to TB and placed for 5 min and 2 hr; T-CNT suspension is stable, compared to U-CNT, c) light microscopic view of the resuspended T-CNT on a slide glass, and d) under polarized light. e) course powder of U-CNT, f) Resuspended U-CNT to TB and placed for 5 min and 2 hr. g) light microscopic view of the resuspended U-CNT on a slide glass, and d) under polarized light. (diameter of the vials in a), b), e) and f) is 2.3 cm)

lysis solution in a centrifuge tube (DNA LoBindid tube 2.0 ml, Eppendorf, Hamburg, Germany) was incubated at 80°C for approx. 24 hr in an oven (HV-100, Funakoshi Co., Ltd., Tokyo, Japan), centrifuged at 20,000 g for 1 hr at 25°C (MX-207, Tomy Seiko Co., Ltd., Tokyo, Japan), and the pellet containing MWCNTs and SDS crystals was recovered. 1.8 ml of 70% ethanol was added to the tube and incubated at 80°C for 30 min to dissolve SDS crystals and centrifuged at 20,000 g for 1 hr at 25°C. 100 µl of 1w/w% Triton®X-100 (MP Biomedicals, Inc., Solon, OH, USA) was added to the pellet and dispersed by pipetting. One microliter of the suspension was placed on an inorganic aluminum oxide membrane filter (Anodisc 13, 0.02 µm φ13mm, Whatman GmbH) or the cellulose acetate/nitrocellulose membrane filter and filtrated on a funnel shape glass filter (SANSYO Co., LTD., Tokyo, Japan). The filter was dried at room temperature and osmium coated for SEM. For a reference of extraction efficiency, lung sample from untreated mouse was spiked with 1 µg T-CNT and measured alongside.

Lung tissue from eight mice were fixed with buffered 10% formalin (four with and four without inflation), paraffin embedded and processed routinely for H&E stained histology slides, and observed under a light microscope with or without polarizing filters (Olympus BX50 microscope with DP-70 image system, Olympus Corporation, Tokyo, Japan).

RESULTS

Characteristics of "Taquann"-dispersed MWCNT

Macroscopic and light microscopic views of the final product, the dried MWCNT after sublimation, i.e. "Taquann"-dispersed MWCNT (T-CNT) and, for comparison, untreated MWCNT from the bulk (U-CNT) are shown in Fig. 4. The powder of T-CNT is finer compared to U-CNT (Fig. 4a). The T-CNT resuspended very well to TB (Fig. 4b) and other solvents including 0.1 w/v% Sodium dodecyl sulfite and 0.1 w/v% Sodium dodecylbenzene sulfonate (not shown). Light microscopically, the resuspended T-CNT consists mostly of dispersed single fibers with smaller numbers of small aggregates corresponding to the mesh size of the metal sieve (Figs. 4c, 4d), whereas U-CNT was a mixture of large aggregates/agglomerates and single fibers among them (Figs. 4g, 4h). The T-CNT fibers slowly precipitated in the medium (cf. Figs. 4b and f), and are easily resuspended by gentle agitation. The yield of the T-CNT was approximately 5% of the U-CNT in weight. Re-filtration of the residue on the sieve resulted in negligible yield. The low power SEM views of the TB-resuspended T-CNT and U-CNT are shown in Fig. 5.

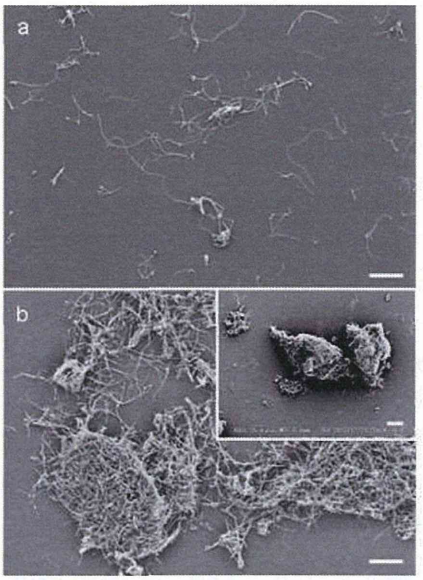

Fig. 5. Scanning electron microscopy of T-CNT and U-CNT resuspended in TB. a) T-CNT consists mainly of dispersed single fibers with few small aggregates/agglomerates smaller than the mesh size of the sieve, SEM x 1,000. b) U-CNT showing mixture of single fibers and large aggregates/agglomerates, SEM x 1,000. The length and width distribution of the single fibers of T-CNT were virtually identical to those of U-CNT. Inset; Lower power view to demonstrate larger aggregates/agglomerates measuring up to 300 μm in major axis SEM x 400. (scale bars are 10 μm)

Again, the majority of the particles of the T-CNT were the dispersed single fibers. The length and width distribution of single fibers counted on these SEM images are shown in Fig. 6. The length and width distribution was similar between single fibers of T-CNT and U-CNT, indicating that the mechanical shortening of the fibers is negligible for Taquann method.

The number of fibers per 10, 1 and 0.1 μg weight of T-CNT with length distribution was counted on SEM images (measured number of fibers are 959, 246, and 45 per designated area for calculation, respectively). The number of fibers calculated was 2.1 x 10^7/10 μg 4.1 x 10^6/1 μg and 3.3 x 10^5/0.1 μg. The distribution of the fiber length was similar to that shown in Fig. 6a, and the average length was 7.5 ± 4.7 μm (max 34 μm), 8.7 ± 6.4 μm (max 42 μm), and 7.0 ± 5.4 μm (max 26 μm) respectively. As a whole, T-CNT has roughly 3 x 10^6 fibers per 1 μg, mean length of approximately 7 μm with a length range up to 50 μm with a median of approximately 6.5 μm.

"Taquann"-dispersed MWCNT in the inhalation chamber

The T-CNT aerosol generated at an average concentration of 1 mg/m^3 was sampled on the Anodisc and observed by a SEM (Fig. 7). The aerosol was composed mainly of well-dispersed single fibers and some small tangles of fibers admixed with a relatively small amount of non-fibrous particles.

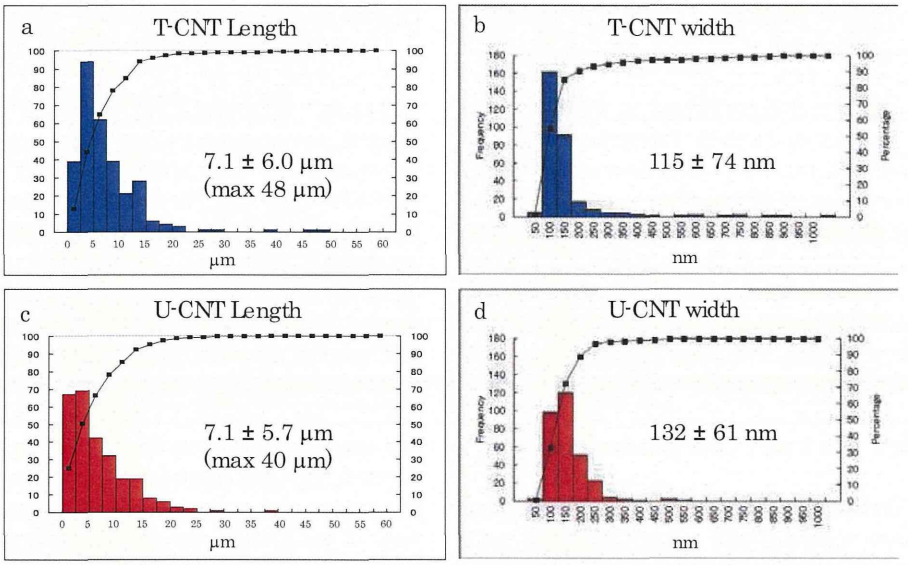

Fig. 6. Length and width of single fibers in T-CNT and U-CNT (measured by SEM on TB-resuspended samples). a) Length distribution and b) width distribution of Taquann-treated MWNT-7. c) Length distribution and d) width distribution of single fibers in the mildly sonicated suspension of the bulk MWNT-7 (mean ± s.d., n = 304 each).

Table 1. Aerosol particle count by optical particle counter (OPC) and condensation particle counter (CPC).

	Date of measurement	2013/4/29	2013/5/1	2013/5/3
Equipment	Mass concentration (mg/m^3)	1.25	1.25	1.38
OPC	Average cpm* (/L) ± s.d.	627,096 ± 145,399	781,973 ± 138,610	821,272 ± 114,278
	K-value (mg/m^3/cpm)	1.99 x 10^{-9}	1.60 x 10^{-9}	1.68 x 10^{-9}
CPC	Average cpm (/L) ± s.d.	859,692 ± 171,858	1,228,545 ± 223,371	1,317,873 ± 217,990
	K-value(mg/m^3/cpm)	1.45 x 10^{-9}	1.02 x 10^{-9}	1.05 x 10^{-9}

*count per minute

Fig. 7. T-CNT aerosol at a concentration of 1 mg/m^3 in the main chamber was collected on the Anodisc filter (5 L/min for 3 min). SEM x 1,000. (scale bar is 10 μm)

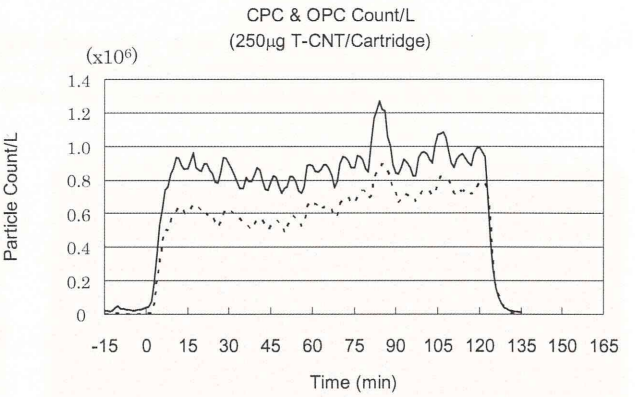

Fig. 8. A real time data from condensation particle counter (CPC, solid line) and optical particle counter (OPC, dotted line) from an inhalation chamber injected with T-CNT (250 μg/cartridge) from 0 min to 120 min with an average injection interval of 6 min (for detail see text).

From the amount of weight increase of polytetrafluoroethylene-glass fiber filter after sampling the chamber aerosol, the weight of aerosol per m^3 of the chamber air (weight concentration) was calculated as approximately 1.3 mg/m^3 (average of three measurements shown in Table 1). At the same time, the particle counts per m^3 given by OPC and CPC were recorded (Fig. 8), and the K-value (mg/particle count in m^3) was calculated (Table 1).

K-value (mg/m^3/cpm), i.e. the weight concentration (mg/m^3) divided by OPC or CPC count per minute (cpm) is often used as an indicator of the status of dispersion. Three measurements conducted with a few days' interval showed that not only the K-values itself but also the values used to calculate it were fairly stable over a period of days.

The length distribution of the T-CNT recovered from the lungs of two mice exposed in the whole body inhalation chamber 2 hr a day for 5 days at an average concentration of 1.8 mg/m^3 of T-CNT are shown in Fig. 9 along with the data from the spiked lung tissue sample. The average length were 8.4 ± 5.0 μm and 8.3 ± 4.9 μm (Figs. 9a, 9b), comparable to that of the T-CNT in spiked lung tissue sample; 9.5 ± 5.2 μm (Fig. 9c) (width was qualitatively not different, data not shown). The total numbers of the fibers recovered were 5.1 x 10^6 and 3.2 x 10^6 from the inhaled lungs and 1.6 x 10^6 from the spiked lung; the weight of T-CNT deposited in the lung after 2 hr x 5 days of inhalation was roughly calculated as 3 μg/lung.

The fibers recovered from one of the mice were observed with SEM (Fig. 10a). Dispersed single fibers were found and some of which are longer that 20 μm (cf. Fig. 9). It was noted that EDTA and ascorbic acid in the lysis solution were effective in removing the debris from the SEM sample (Fig. 10b).

Histologically, the CNTs were found to distribute from bronchial lumen to peripheral alveolar spaces. In the bronchial lumen, the fibers were trapped in the bronchial mucus, either as single fibers or as loose aggregates

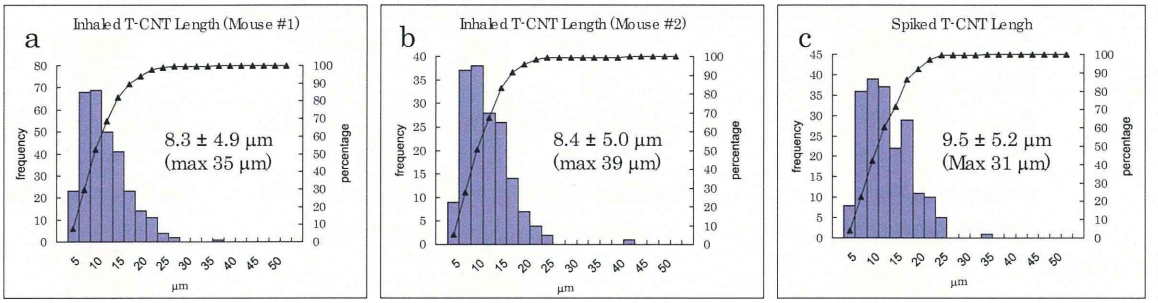

Fig. 9. T-CNT recovered from the mouse lung. a, b) Length distribution of T-CNT in the lung of two mice exposed 2 hr a day for 5 days at an average concentration of 1.8 mg/m^3 (n = 306 and 166 each, mean ± s.d). c) Length distribution of T-CNT (1 μg) spiked to a non-exposed mouse lung (n = 198, mean ± s.d).

Fig. 10. T-CNT recovered from the mouse lung. a) SEM of the sediment of the dissolved lung of a mouse exposed to T-CNT in an inhalation chamber 2 hr a day for 5 days, x 2,000. Long and short single fibers are shown to be inhaled (treated with solution containing EDTA and ascorbic acid). b) SEM of a same sample treated without EDTA and ascorbic. The debris covering the fibers is considered to be iron-based amorphous substances soluble to EDTA, x 2,000. Ascorbic acid was found to be effective in keeping iron ions to be bivalent (ferrous) and soluble. (scale bars are 10 μm)

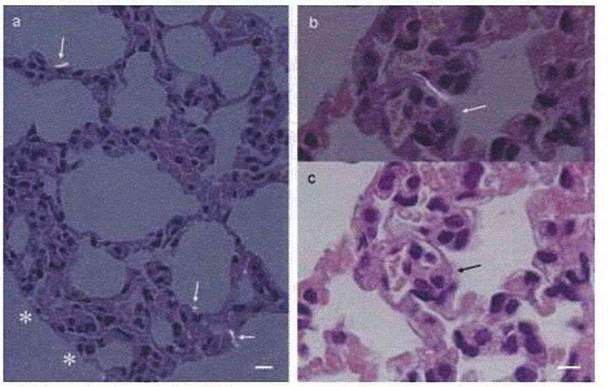

Fig. 11. a) A polarized microscopic view of the alveolar region of a lung exposed to 1 mg/m^3 of T-CNT for 2 hr a day for 5 days. Arrows indicate single T-CNTs deposited in alveolar spaces phagocytized by alveolar macrophages. Asterisks indicates visceral pleural. (scale bar 10 μm) b,c) Another portion of alveolar region with a tadpole-shaped alveolar macrophage containing single long CNT in its cytoplasm shown in plain and polarized view. The lungs shown here are not inflated with formalin at fixation in order to avoid replacement of the CNTs. (scale bar 5 μm)

without inflammatory or granulomatous response, morphologically interpretable as a view of expectoration by the ciliary movement of the bronchial epithelium. There were no dense aggregates/agglomerates in the lungs so far as examined. In the peripheral alveolar space, single fibers are found phagocytized in alveolar macrophages as shown in Fig. 11. There were only mild inflammatory reactions such as neutrophilic migration against fibers in mucous blanket of the bronchial/bronchiolar segments and fibers in the alveolar space.

DISCUSSION

The MWCNT treated with the "Taquann" method (T-CNT) consisted of highly dispersed single fibers with marked reduction of aggregates/agglomerates, both in the aerosol and in the resuspended solution. The length and width distribution of the single fibers were not different between the T-CNT and the original U-CNT, indicating that this method is physically mild to the sample and does not shorten the fibers.

The Taquann method consists of two major steps, the